

Published in final edited form as:

*Nature*. 2013 February 14; 494(7436): 243–246. doi:10.1038/nature11823.

## A direct and melanopsin-dependent fetal light response regulates mouse eye development

Sujata Rao<sup>1</sup>, Christina Chun<sup>2</sup>, Jieqing Fan<sup>1</sup>, J. Matthew Kofron<sup>3</sup>, Michael B. Yang<sup>1,4</sup>, Rashmi S. Hegde<sup>3</sup>, Napoleone Ferrara<sup>5</sup>, David R. Copenhagen<sup>2</sup>, and Richard A. Lang<sup>1,3,4</sup>

<sup>1</sup>The Visual Systems Group, Abrahamson Pediatric Eye Institute, Division of Pediatric Ophthalmology, Cincinnati Children's Hospital Medical Center, Cincinnati, Ohio 45229, USA

<sup>2</sup>Departments of Ophthalmology and Physiology, University of California, San Francisco, San Francisco, California 94158, USA

<sup>3</sup>The Division of Developmental Biology, Cincinnati Children's Hospital Medical Center, Cincinnati, Ohio 45229, USA

<sup>4</sup>Department of Ophthalmology, University of Cincinnati, College of Medicine, Cincinnati, Ohio 45229, USA

<sup>5</sup>Genentech Inc., 1 DNA Way, South San Francisco, California 94080, USA

### Abstract

Vascular patterning is critical for organ function. In the eye, there is simultaneous regression of embryonic hyaloid vasculature<sup>1</sup> (important to clear the optical path) and formation of the retinal vasculature<sup>2</sup> (important for the high metabolic demands of retinal neurons). These events occur postnatally in the mouse. Here we have identified a light-response pathway that regulates both processes. We show that when mice are mutated in the gene (*Opn4*) for the atypical opsin melanopsin<sup>3–5</sup>, or are dark-reared from late gestation, the hyaloid vessels are persistent at 8 days post-partum and the retinal vasculature overgrows. We provide evidence that these vascular anomalies are explained by a light-response pathway that suppresses retinal neuron number, limits hypoxia and, as a consequence, holds local expression of vascular endothelial growth factor (VEGFA) in check. We also show that the light response for this pathway occurs in late gestation at about embryonic day 16 and requires the photopigment in the fetus and not the mother. Measurements show that visceral cavity photon flux is probably sufficient to activate melanopsin-expressing retinal ganglion cells in the mouse fetus. These data thus show that light—the stimulus for function of the mature eye—is also critical in preparing the eye for vision by regulating retinal neuron number and initiating a series of events that ultimately pattern the ocular blood vessels.

Prompted by the recognition that newborn mice are light-responsive<sup>6</sup> and show light-dependent neuronal connectivity changes<sup>7</sup>, we proposed the existence of a pathway in which light responsiveness in the early retina might trigger hyaloid regression and thus clearance of

a. ©2013 Macmillan Publishers Limited. All rights reserved

Author Information Reprints and permissions information is available at [www.nature.com/reprints](http://www.nature.com/reprints). The authors declare competing financial interests: details are available in the online version of the paper. Readers are welcome to comment on the online version of the paper. Correspondence and requests for materials should be addressed to R.A.L. ([richard.lang@cchmc.org](mailto:richard.lang@cchmc.org)) or D.R.C. ([cope@phy.ucsf.edu](mailto:cope@phy.ucsf.edu)).

**Supplementary Information** is available in the online version of the paper

**Author Contributions** R.A.L. and D.R.C. provided project leadership. R.A.L., D.R.C. and S.R. wrote the manuscript. R.A.L., D.R.C. and R.S.H. supervised experimental work. N.F. developed critical reagents and M.B.Y. provided important clinical insights. S.R., C.C., J.F., J.M.K. and D.R.C. performed experimentation and analysis.

the optic axis. To test this, we placed pregnant dams in the dark at late gestation (embryonic (E) day 16–17): pups raised in the dark until 8 days post partum (P8) showed persistent hyaloid vessels (Fig. 1a) and this was confirmed by quantification over a P1–P8 time course (Fig. 1b). Assessment of hyaloid vessel numbers at P15 showed that by this stage they had regressed. This indicated that dark-rearing resulted in a regression delay. Quantification of apoptosis at P5 showed that regardless of whether we quantified the isolated events that predominate early in hyaloid regression or the segmental pattern of apoptosis that follows<sup>8</sup>, there was a reduction (Fig. 1c) similar quantitatively to previously characterized hyaloid persistence mutants<sup>9</sup>. These data suggest that a light-response pathway promotes hyaloid regression.

Hyaloid vessel regression and superficial layer retinal angiogenesis occur at the same time in the mouse<sup>1,10</sup>, and this indicated that dark-rearing might affect both processes. Retinal angiogenesis in mice begins at the day of birth with the extension of vessel precursors from the head of the optic nerve. A superficial layer of vasculature within the retinal ganglion cell (RGC) layer extends to the retinal periphery by P7 (Supplementary Fig. 1a–c). Starting at about P8, angiogenic sprouts extend vertically downwards into the deeper layers of the retina (Supplementary Fig. 1d) and ultimately form the deep vasculature at the outer edge of the inner nuclear layer and the intermediate plexus within the inner plexiform layer<sup>2</sup>. In mice dark-reared from E16 to E17, the superficial vascular plexus (Supplementary Fig. 1e) showed an increase in density regardless of whether the region was simple plexus (Supplementary Fig. 1f) or at a vein (Supplementary Fig. 1g). Depth-coded P8 image stacks (Supplementary Fig. 1h) showed that there were many more descending vessels (Supplementary Fig. 1h, yellow, blue) than in the wild type (Supplementary Fig. 1h, yellow) and many of these were abnormally located. These changes were confirmed by quantification (Supplementary Fig. 1i, j). Thus, the retinal vasculature is a second vascular structure in the eye where normal development is disrupted by the absence of light.

Melanopsin is expressed from an early stage of both mouse and human gestation and unlike photoreceptor opsins, is known to function in the mouse eye before P10 (ref. 11). Melanopsin-expressing intrinsically photosensitive retinal ganglion cells (ipRGCs) are a subset of RGCs that function in circadian entrainment and the pupillary reflex<sup>12</sup>. ipRGCs are located in the superficial layers of the retina adjacent to both the retinal and hyaloid vasculatures (Supplementary Fig. 2a–c). This location, the pre-photoreceptor functions of melanopsin<sup>6</sup> and the vascular anomalies present in mice that are missing RGCs<sup>13</sup>, suggested that it was a good candidate to mediate light-dependent vascular development in the eye. To test this possibility, we assessed hyaloid vessel regression and retinal vascular development in mice mutated in *Opn4*, the melanopsin-encoding gene<sup>4,5</sup>. *Opn4*<sup>-/-</sup> mice showed normal hyaloid vessel numbers at P1 but persistence at P8 (Fig. 2a and Supplementary Fig. 2d). Examination of P15 eyes showed that hyaloid regression was complete in the *Opn4*<sup>-/-</sup> mice, indicating that, as with dark-reared mice, hyaloid persistence was not long term. *Opn4*<sup>-/-</sup> mice also showed a retinal vascular overgrowth phenotype that qualitatively and quantitatively (Fig. 2b–k) mimicked the changes resulting from dark rearing. To determine whether changes in retinal vascular density endured, we performed a quantitative assessment at P15, P25 and P180 (Supplementary Fig. 3) that showed that elevated vascular density was regionally sustained until at least P180. More generally, the vascular phenotype of the *Opn4*<sup>-/-</sup> mice phenocopies that observed in dark-reared mice. This provides an independent means of implicating a light-response pathway in vascular development of the eye and identifies melanopsin as the opsin required.

VEGFA is a potent signal for vascular endothelial cell survival<sup>14</sup> that is required for retinal angiogenesis<sup>15</sup> and is also present in the vitreous of the rodent<sup>16</sup> and human<sup>17</sup> eye where the hyaloid vessels reside. We proposed that light-dependent vascular development might be

explained by modulation of VEGFA. Consistent with this, homozygous and heterozygous deletion of *Vegfa*<sup>fl</sup> with the *Chx10-cre* retinal driver<sup>18</sup> gave, respectively, either a hyaloid development failure (Supplementary Fig. 4a) or diminished hyaloid regression (Fig. 3a and Supplementary Fig. 4b). An immunoblot for vitreous VEGFA over the P1–P8 time course revealed that in control mice, VEGFA164 levels were reduced at P5 but rose again by P8 (Fig. 3b). When three different time courses of VEGFA immunoblots were quantified, the P5 VEGFA signal was about fivefold reduced compared with P1 (Fig. 3b). A low level of VEGFA at P5 is consistent with the idea that it is a key regulator of hyaloid regression because P5 is the time when there are peak levels of vascular endothelial cell apoptosis<sup>9</sup>.

Using dark rearing and the *Opn4*<sup>-/-</sup> mice, we determined whether actual or functional darkness resulted in a modulation of vitreous VEGFA. In four independent experiments we consistently observed that vitreous VEGFA levels were increased regardless of how light responsiveness was compromised (Fig. 3c). Furthermore, an enzyme-linked immunosorbent assay (ELISA)-based assessment of VEGFA in the P5 vitreous showed that whether pups were dark-reared or mutated in *Opn4*, the levels of VEGFA were about sevenfold higher than in the control (Fig. 3d). A sevenfold increase in VEGFA in the vitreous of dark-reared and *Opn4*<sup>-/-</sup> mice was reflected in similar fold increases in the level of retinal *Vegfa* messenger RNA as indicated by quantitative polymerase chain reaction (qPCR) (Fig. 3e). Flow sorting/qPCR further showed that Thy1.1<sup>+</sup> RGCs and Thy1.1<sup>-</sup>Vc1.1<sup>+</sup> amacrine/horizontal cells exhibited an increase in *Vegfa* mRNA, although Thy1.1<sup>-</sup>Vc1.1<sup>-</sup>PDGFR<sup>+</sup> astrocytes did not (Supplementary Fig. 5a). Given the VEGFA dependence of hyaloid vessels (Supplementary Fig. 4) and of retinal angiogenesis<sup>15</sup>, elevated retinal VEGFA expression is an explanation for the vascular anomalies observed in dark-reared and *Opn4*<sup>-/-</sup> mice.

Quantification of BRN3B<sup>+</sup> RGCs and calretinin<sup>+</sup> amacrine cells in P5 *Opn4*<sup>-/-</sup> mice revealed modest increases in the numbers of both cell types (Supplementary Fig. 5d). It has been shown that retinal angiogenesis in the mouse is driven by a hypoxia-response pathway that upregulates VEGFA expression<sup>19,20</sup>. Because increased cell number can increase oxygen demand, we tested whether the *Opn4* mutation and dark rearing resulted in retinal hypoxia (Fig. 3f, g). Quantification of labelling with hypoxyprobe at P5 (Fig. 3h, i) revealed that increased signal was a consequence of both *Opn4* mutation and dark rearing. This is consistent with the hypothesis that elevated VEGFA expression in the retina is a consequence of increased oxygen demand due to higher numbers of retinal neurons (Supplementary Fig. 7).

In assessing the role of light responses in vascular development of the eye, our presumption had been that birth was probably a triggering event because vascular patterning events occur after birth and because light levels to the eye of the newborn would increase. To test this, we dark-reared pups from different points of late gestation (E16–17, E17–E18 or after E18) and assessed hyaloid persistence. We observed a dose response where the hyaloid vessels were progressively more persistent with an earlier dark-rearing start (Fig. 4a). In particular, if dark rearing was started after E18 (the day of birth is usually E19) there was almost no effect (Fig. 4a, light blue bar). These data indicate the surprising outcome that the critical light-response period stimulating hyaloid regression is gestational, at or before E16–17. This further raised the possibility that this developmental pathway required a direct fetal light response. To test this assertion directly, we transferred embryos from an *Opn4*<sup>+/-</sup> × *Opn4*<sup>+/-</sup> cross into a pseudopregnant wild-type female and assessed hyaloid regression. Control, wild-type pups in the transferred litter showed normal hyaloid regression (Fig. 4d, b, grey bar), whereas the *Opn4*<sup>-/-</sup> mice showed persistence at P8 (Fig. 4d, c, blue bar). In addition, to test the reciprocal possibility—that the light response of the mother might influence vascular development of the fetal eye—we enucleated female mice, and allowed them to

gestate and raise litters under normal lighting conditions. This did not produce hyaloid persistence (Fig. 4d). Combined, these experiments show that melanopsin in the fetus, not the mother, is critical to regulate vascular development of the eye.

Measurements of the light level in the visceral cavity of adult mice living under mouse room fluorescent lights (Supplementary Fig. 6) revealed flux densities of  $1.4 \times 10^{13}$  (for BALB/c) and  $1.1 \times 10^{12}$  (for C57BL/6) photons  $\text{cm}^{-2} \text{s}^{-1}$ . Published response thresholds for rodent ipRGCs range upwards from approximately  $1.2 \times 10^{10}$  photons  $\text{cm}^{-2} \text{s}^{-1}$  (refs 21–23). Furthermore, it has been shown that ipRGCs have the ability to respond continuously to light stimulation, via melanopsin, for up to 10 h (ref. 23). Although it has been suggested that ipRGCs in newborn mouse pups are less sensitive than in adults<sup>22</sup>, the reduced sensitivity is about 1.5 log quanta and so the visceral light level in a pigmented animal of  $1.1 \times 10^{12}$  photons  $\text{cm}^{-2} \text{s}^{-1}$  may still be above the threshold. These data are consistent with the hypothesis that the mouse fetus can respond directly to light via melanopsin.

These experimental studies identify light as a trigger for hyaloid vessel regression and for suppression of promiscuous angiogenesis in the retina. The observation that dark rearing from late gestation or *Opn4* mutation produces essentially identical perturbations of vascular development provides corroborating evidence for involvement of a melanopsin-dependent, light-response pathway (Supplementary Fig. 7). Our data also indicate that the origin of the hyaloid persistence and de-regulated retinal angiogenesis is increased levels of VEGFA originating in retinal neurons. These findings are surprising because, with the exception of neuronal connectivity, it has not been shown previously that light can trigger changes in developmental programs. Our data indicate that the primary light-dependent change is an increase in the number of retinal neurons and that the vascular changes occur in response to increased oxygen demand (Supplementary Fig. 7) considerably later in developmental time. This pathway is an interesting example of one where events unfold slowly over the course of nearly 2 weeks. It will be interesting to determine whether this pathway might influence susceptibility to retinopathy of pre-maturity<sup>24</sup>, the retinal vasculopathy of pre-term infants in which promiscuous angiogenesis can cause blindness.

## 2. Methods

### a. Mice

Genotyping of *Vegfa*<sup>f1</sup> (ref. 26), *Chx10-cre* (ref. 18), *Opn4*<sup>cre</sup> (ref. 27), *Ai4* (ref. 28) and *Opn4*<sup>-/-</sup> (ref. 5) was performed as described. All animal experimentation was carried out using protocols approved by the Institutional Animal Care and Use Committee at Cincinnati Children's Hospital Medical Center and at the University of California San Francisco.

### b. Hyaloid and retinal labelling and quantification

Hyaloid vessels were collected and stained with Hoechst as well as for TdT-mediated dUTP nick end labelling (TUNEL) as described<sup>9</sup>. Retinal flat-mounts were prepared and labelled with isolectin<sup>29</sup> or for melanopsin<sup>4</sup>. Hyaloid vessel quantification has been described previously<sup>1</sup>. Retinal vessel density was quantified by counting vessel junctions using ImageJ for many  $\times 200$  microscope fields. Depth-coded three-dimensional image reconstructions were generated using a Zeiss Apotome-equipped microscope in conjunction with Axiovision software. Antibodies for labelling of retinal flat-mounts included anti-Brn3b (Abcam), anti-calretinin (Millipore) and anti-melanopsin (ATS).

### c. Assessment of hypoxia

P5 mouse pups were injected with  $60 \text{ mg kg}^{-1}$  (about  $180 \mu\text{g}$  per pup) pimonidazole hydrochloride (Hypoxyprobe), and after 45 min were killed and retinas collected. The rabbit

primary antibody to pimonidazole hydro-chloride was then used in conjunction with an anti-rabbit Alexa594 secondary to label retinal tissue. We quantified labelling by generating intensity values along line intervals extending from the retinal centre to the periphery. Pixel intensity values from 20 to 25 line intervals per retina and 5 to 6 retinas per genotype were averaged. Significance values were calculated using the MatLab ANOVA test.

#### d. Isolation and analysis of vitreous

Vitreous was collected from dark-reared pups in a room using red illumination. Eyes from P1 and P5 pups were washed twice in sterile ice cold PBS. Excess PBS was blotted using a kimwipe, a small slit was made through the retina and vitreous collected. ELISA was performed on the vitreous using the Vegfa Quantikine kits (R&D) that include recombinant protein standards. Immunoblots were probed with a unique carboxy-terminal antibody for VEGFA<sup>30</sup> from Santa Cruz. Quantification was performed using ImageJ.

#### e. Cell sorting

For flow sorting using markers for retinal neurons<sup>31</sup>, retina was dissociated as described<sup>25</sup> except 16 mg ml<sup>-1</sup> of liberase CI (Roche) and 20µg ml<sup>-1</sup> of DNase I (Sigma) was used. Cells were then labelled on ice for 30 min with goat PDGFR- $\alpha$ , washed with PBS and labelled with PerCP-conjugated anti-CD90 (clone OX-7), FITC-conjugated anti-CD57 (clone VC1.1), Alexa fluor 350 and 7-AAD. Cells were sorted with FACSARIA II running DiVa software.

#### f. RNA isolation and qPCR

RNA was isolated using RNeasy (Qiagen). qPCR was performed with QuantiTect SYBR green (Qiagen) using amplification of actin for normalization. In analysing qPCR data, the P values refer to a comparison of the  $\Delta\Delta CT$  values. Primers were as follows: *Vegfa* 5' - GACAGAACAAAGCCAGA-3', 5' - CACCGCCTTGGCTTGTCAC-3'.

#### g. Light measurements

To estimate the radiant flux density impinging a mouse housed in a cage in the UCSF animal care facilities, we determined the spectral distribution of fluorescent lights,  $S(\lambda_{\text{relative}})$ , illuminating the room and the absolute power (watts cm<sup>-2</sup>s<sup>-1</sup>) of these lights. Both measurements were done at floor level.  $S(\lambda_{\text{relative}})$  was measured (Photo Research, PR670 spectroradiometer) as light reflected from a spectrally flat reflective surface (Spectralon Target, Labsphere). The radiant power was measured using a calibrated radiometric detector (UDT Instruments; model S471).  $S(\lambda_{\text{relative}})$  was converted to  $S(\lambda_{\text{absolute}})$  by scaling the area under  $S(\lambda_{\text{relative}})$  to match the radiant power and then converting these values to photons cm<sup>-2</sup>s<sup>-1</sup> for each wavelength. The melanopsin spectral absorbance curve was then convolved with  $S(\lambda_{\text{absolute}})$ . The area under this curve was used as a measure of the radiant flux density capable of stimulating the melanopsin pigment ( $\lambda_{\text{max}} = 479$  nm). We calculate that the equivalent of at least  $5 \times 10^{13}$  photons cm<sup>-2</sup> s<sup>-1</sup> was available to stimulate melanopsin. Similar measurements and calculations for sunlight (12:00, 20 December 2011) revealed a radiant flux density of  $2.6 \times 10^{16}$  photons cm<sup>-2</sup>s<sup>-1</sup>.

To estimate attenuation of light that could stimulate melanopsin in mouse fetuses in *utero*, we directed a blue LED (Philips Lumileds Lighting Company; model: Luxeon III star, LXHL-LB3C, peak wavelength = 470 nm) that was positioned 1 inch from the skin to a miniature silicon photodiode light detector placed inside the abdominal cavity. Light penetrated both the skin and sub-dermal muscle layer. The measurements were done on live, anaesthetized adult mice (intramuscular (IM) injections of ketamine/xylazine).

## Supplementary Material

Refer to Web version on PubMed Central for supplementary material.

## Acknowledgments

We thank D. Bredl, P. Speeg and M. Sarangdhar for technical assistance, A. Delwig and N. Brown for advice. We acknowledge the assistance of the Research Flow Cytometry Core in the Division of Rheumatology at CCHMC, supported in part by NIH AR-47363. This work was supported by the NIH (R.A.L., D.R.C., J.M.K. and R.S.H.) with additional funding from the Abrahamson Pediatric Eye Institute of CCHMC, That Man May See at UCSF, Research to Prevent Blindness (D.R.C.) and March of Dimes (D.R.C.).

## References

1. Ito M, Yoshioka M. Regression of the hyaloid vessels and pupillary membrane of the mouse. *Anat Embryol (Berl)*. 1999; 200:403–411. [PubMed: 10460477]
2. Fruttiger M. Development of the retinal vasculature. *Angiogenesis*. 2007; 10:77–88. [PubMed: 17322966]
3. Provencio I, Jiang G, De Grip WJ, Hayes WP, Rollag MD. Melanopsin: an opsin in melanophores, brain, and eye. *Proc Natl Acad Sci USA*. 1998; 95:340–345. [PubMed: 9419377]
4. Hattar S, Liao HW, Takao M, Berson DM, Yau KW. Melanopsin-containing retinal ganglion cells: architecture, projections, and intrinsic photosensitivity. *Science*. 2002; 295:1065–1070. [PubMed: 11834834]
5. Panda S, et al. Melanopsin (*Opn4*) requirement for normal light-induced circadian phase shifting. *Science*. 2002; 298:2213–2216. [PubMed: 12481141]
6. Johnson J, et al. Melanopsin-dependent light avoidance in neonatal mice. *Proc Natl Acad Sci USA*. 2010; 107:17374–17378. [PubMed: 20855606]
7. Tian N, Copenhagen DR. Visual stimulation is required for refinement of ON and OFF pathways in postnatal retina. *Neuron*. 2003; 39:85–96. [PubMed: 12848934]
8. Diez-Roux G, Lang RA. Macrophages induce apoptosis in normal cells *in vivo*. *Development*. 1997; 124:3633–3638. [PubMed: 9342055]
9. Lobov IB, et al. WNT7b mediates macrophage-induced programmed cell death in patterning of the vasculature. *Nature*. 2005; 437:417–421. [PubMed: 16163358]
10. Saint-Geniez M, D'Amore PA. Development and pathology of the hyaloid, choroidal and retinal vasculature. *Int J Dev Biol*. 2004; 48:1045–1058. [PubMed: 15558494]
11. Tarttelin EE, et al. Expression of opsin genes early in ocular development of humans and mice. *Exp Eye Res*. 2003; 76:393–396. [PubMed: 12573668]
12. Do MT, Yau KW. Intrinsically photosensitive retinal ganglion cells. *Physiol Rev*. 2010; 90:1547–1581. [PubMed: 20959623]
13. Edwards MM, et al. The deletion of *Math5* disrupts retinal blood vessel and glial development in mice. *Exp Eye Res*. 2012; 96:147–156. [PubMed: 22200487]
14. Ferrara N, Gerber HP, LeCouter J. The biology of VEGF and its receptors. *Nature Med*. 2003; 9:669–676. [PubMed: 12778165]
15. Haigh JJ, et al. Cortical and retinal defects caused by dosage-dependent reductions in VEGF-A paracrine signaling. *Dev Biol*. 2003; 262:225–241. [PubMed: 14550787]
16. Meeson AP, Argilla M, Ko K, Witte L, Lang RA. VEGF deprivation-induced apoptosis is a component of programmed capillary regression. *Development*. 1999; 126:1407–1415. [PubMed: 10068634]
17. Adamis AP, et al. Increased vascular endothelial growth factor levels in the vitreous of eyes with proliferative diabetic retinopathy. *Am J Ophthalmol*. 1994; 118:445–450. [PubMed: 7943121]
18. Rowan S, Cepko CL. Genetic analysis of the homeodomain transcription factor *Chx10* in the retina using a novel multifunctional BAC transgenic mouse reporter. *Dev Biol*. 2004; 271:388–402. [PubMed: 15223342]

19. Kurihara T, et al. von Hippel-Lindau protein regulates transition from the fetal to the adult circulatory system in retina. *Development*. 2010; 137:1563–1571. [PubMed: 20388654]
20. Lange C, et al. Retina-specific activation of a sustained hypoxia-like response leads to severe retinal degeneration and loss of vision. *Neurobiol Dis*. 2010; 41:119–130. [PubMed: 20817091]
21. Sekaran S, et al. Melanopsin-dependent photoreception provides earliest light detection in the mammalian retina. *Curr Biol*. 2005; 15:1099–1107. [PubMed: 15964274]
22. Tu DC, et al. Physiologic diversity and development of intrinsically photosensitive retinal ganglion cells. *Neuron*. 2005; 48:987–999. [PubMed: 16364902]
23. Wong KY. A retinal ganglion cell that can signal irradiance continuously for 10 hours. *J Neurosci*. 2012; 32:11478–11485. [PubMed: 22895730]
24. Connor KM, et al. Quantification of oxygen-induced retinopathy in the mouse: a model of vessel loss, vessel regrowth and pathological angiogenesis. *Nature Protocols*. 2009; 4:1565–1573.
25. Stefater JA, et al. Regulation of angiogenesis by a non-canonical Wnt–Flt1 pathway in myeloid cells. *Nature*. 2011; 474:511–515. [PubMed: 21623369]
26. Lichtenberger BM, et al. Autocrine VEGF signaling synergizes with EGFR in tumor cells to promote epithelial cancer development. *Cell*. 2010; 140:268–279. [PubMed: 20141840]
27. Ecker JL, et al. Melanopsin-expressing retinal ganglion-cell photoreceptors: cellular diversity and role in pattern vision. *Neuron*. 2010; 67:49–60. [PubMed: 20624591]
28. Madisen L, et al. A robust and high-throughput Cre reporting and characterization system for the whole mouse brain. *Nature Neurosci*. 2010; 13:133–140. [PubMed: 20023653]
29. Gerhardt H, et al. VEGF guides angiogenic sprouting utilizing endothelial tip cell filopodia. *J Cell Biol*. 2003; 161:1163–1177. [PubMed: 12810700]
30. Stockmann C, et al. Deletion of vascular endothelial growth factor in myeloid cells accelerates tumorigenesis. *Nature*. 2008; 456:814–818. [PubMed: 18997773]
31. Goldberg JL, Klassen MP, Hua Y, Barres BA. Amacrine-signaled loss of intrinsic axon growth ability by retinal ganglion cells. *Science*. 2002; 296:1860–1864. [PubMed: 12052959]

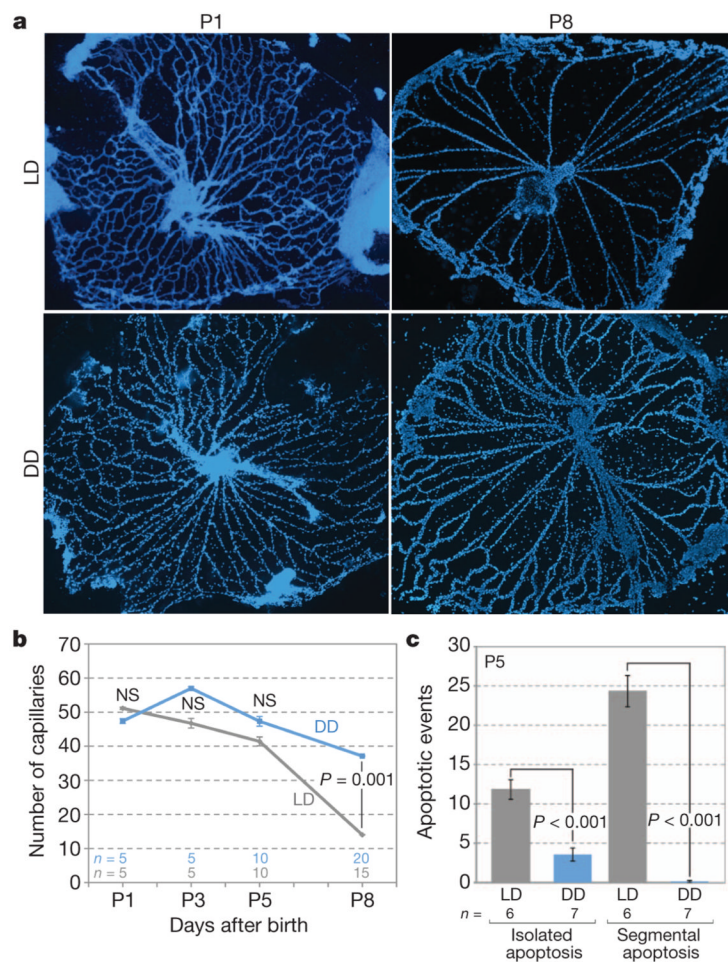


**Figure 1. | Hyaloid regression is regulated by light**

**a**, Hyaloid vessel preparations at the indicated postnatal (P) days from pups reared under normal light conditions (LD) or under constant darkness (DD) from E16–17. Original magnification,  $\times 50$ . **b**, As in **a** but a quantification of vessel number from P1 to P8.  $P$  values obtained by analysis of variance (ANOVA). **c**, P5 apoptotic index in hyaloid vascular cells (isolated apoptosis) or vessels undergoing a segmental pattern of apoptosis.  $P$  values obtained by Student's  $t$ -test. Sample size ( $n$ ) as labelled. NS, not significant. Error bars are s.e.m.



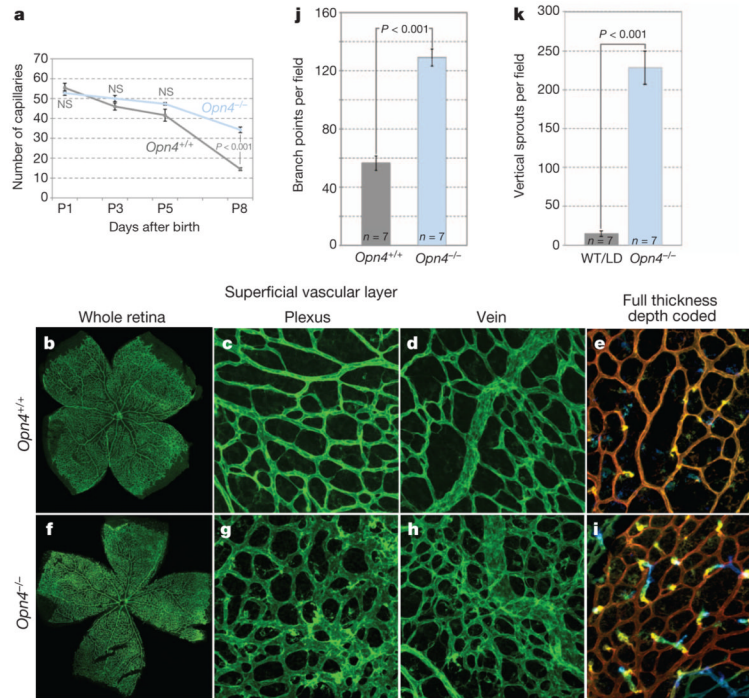


**Figure 2. |Hyaloid regression and retinal angiogenesis are regulated by melanopsin**  
**a**, Quantification of hyaloid vessels in *Opn4<sup>+/+</sup>* and *Opn4<sup>-/-</sup>* mice over a P1 to P8 time course. *P* values obtained by ANOVA. **b–i**, Low ( $\times 100$ ; **b, f**) and high ( $\times 200$ ; **c–e, g–i**) magnification images of isolectin-labelled P8 retina from wild-type (**b–e**) and *Opn4<sup>-/-</sup>* (**f–i**) pups raised in normal lighting. **e, i**, Depth-coded z stack images for wild type (**e**) and *Opn4<sup>-/-</sup>* (**i**) indicate the appearance of vertical angiogenic sprouts. **j, k**, Graphs show quantification of branch points (**j**) and vertical sprouts (**k**) in animals of the indicated genotypes. WT, wild type. *P* values obtained by Student's *t*-test. Errors bars are s.e.m. Sample sizes (*n*) as labelled.

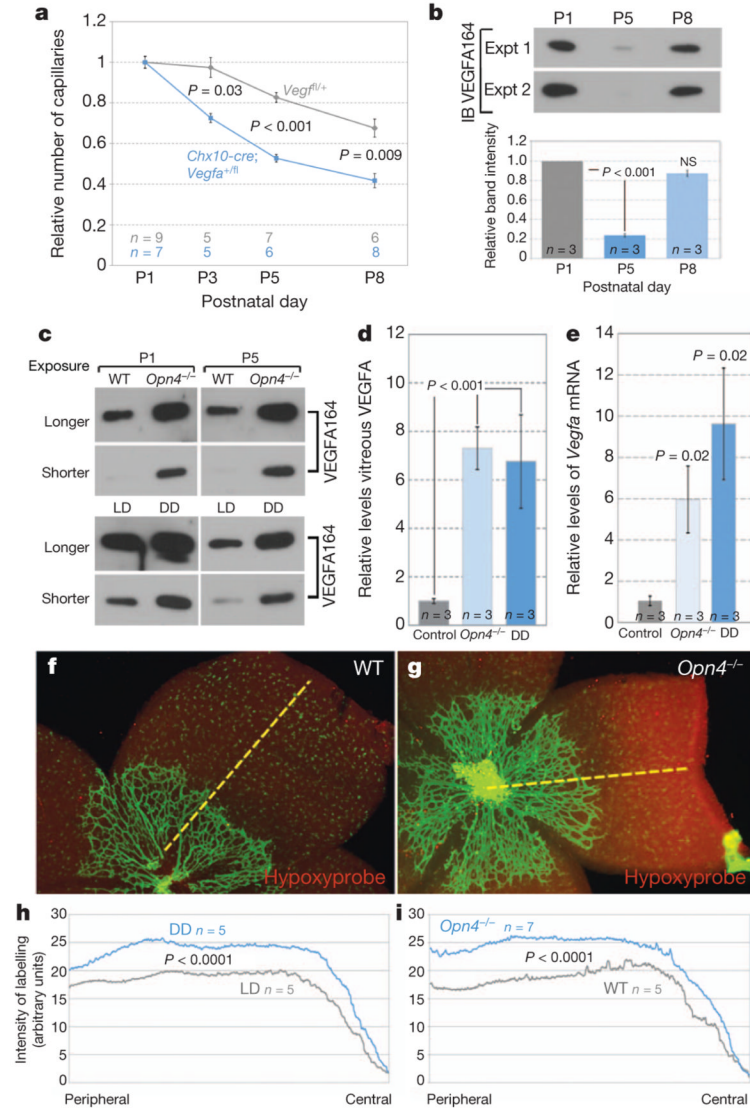


**Figure 3. | Light and melanopsin-dependent regulation of VEGFA expression and hypoxia in the retina**

**a**, Hyaloid vessel number from P1 to P8 in mice of labelled genotypes. *P* values obtained by ANOVA. **b**, Vitreous VEGFA immunoblot (IB) for wild-type mice at P1, P5 and P8 with quantification histogram. **c**, Immunoblot for P1 or P5 vitreous VEGFA in wild-type and *Opn4*<sup>-/-</sup> mice or in mice reared in LD or DD light conditions as labelled. **d**, ELISA quantification of VEGFA levels in the P5 vitreous of control/LD mouse pups (grey bar) from *Opn4*<sup>-/-</sup> mice (pale blue bar) or those raised in constant darkness from E16–17 (DD, blue bar). **e**, qPCR detection of *Vegfa* mRNA in P5 retina from control/LD (grey bar), *Opn4*<sup>-/-</sup> mice (light blue bar) and dark-reared mice (DD, dark blue bar). *P* values in **b**, **d**, **e** were obtained by Student's *t*-test. Sample sizes (*n*) as labelled. Error bars are s.e.m. **f**, **g**, Labelling of flat-mount P5 retinas from wild-type (**f**) and *Opn4*<sup>-/-</sup> (**g**) mice for blood vessels (isolectin, green) and for hypoxia (red). Retinal myeloid cells label faintly with isolectin. Original magnification, ×100. **h**, **i**, Quantification of the relative levels of hypoxyprobe labelling in the retinas of LD and DD mice (**c**) and wild-type versus *Opn4*<sup>-/-</sup> (**d**) retinas.

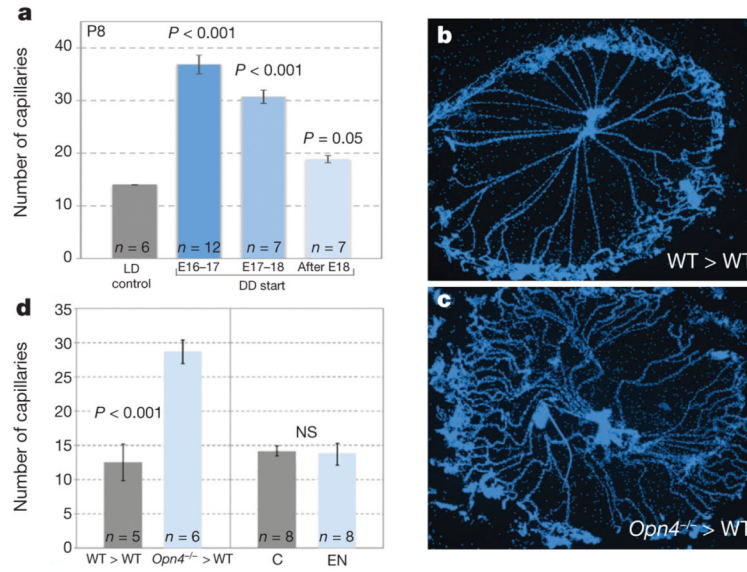


**Figure 4. | Gestational light controls vascular development in the eye**

**a**, Quantification of hyaloid vessels in mice raised in normal lighting (LD, grey bar) and those dark-reared from E16–17 (dark-blue bar), E17–18 (medium-blue bar), or after E18 (light-blue bar). **b**, **c**, P8 hyaloid vessel preparations from a wild-type embryo transferred into a wild-type pseudopregnant female (WT>WT) and an *Opn4<sup>-/-</sup>* embryo transferred into a wild-type pseudopregnant female (*Opn4<sup>-/-</sup>* > WT). Original magnification,  $\times 50$ . **d**, Left panel: quantification of hyaloid vessels in P8 WT>WT ( $n = 5$ ) and *Opn4<sup>-/-</sup>*>WT ( $n = 6$ ) pups. Right panel: quantification of hyaloid vessels in normal control pups at P8 (C;  $n = 8$ ) and P8 pups ( $n = 8$ ) born to an enucleated female (EN). Sample sizes ( $n$ ) as labelled.  $P$  values in **a** by ANOVA;  $P$  values in **d** were obtained by Student's  $t$ -test. Errors bars are s.e.m.